Three Different Phenotypes of Mild Nonproliferative Diabetic Retinopathy With Different Risks for Development of Clinically Significant Macular Edema

Sandrina Nunes,[1,2] Luisa Ribeiro,[1,2] Conceição Lobo,[1,2] and José Cunha-Vaz[1,2]

[1]Association for Innovation and Biomedical Research on Light and Image (AIBILI), Coimbra, Portugal
[2]Faculty of Medicine, University of Coimbra, Coimbra, Portugal

Correspondence: José Cunha-Vaz, AIBILI, Azinhaga de Santa Comba – Celas, 3000-548 Coimbra, Portugal; cunhavaz@aibili.pt.

Submitted: February 19, 2013
Accepted: May 28, 2013

Citation: Nunes S, Ribeiro L, Lobo C, Cunha-Vaz J. Three different phenotypes of mild nonproliferative diabetic retinopathy with different risks for development of clinically significant macular edema. *Invest Ophthalmol Vis Sci*. 2013;54:4595–4604. DOI: 10.1167/iovs.13-11895

Purpose. To identify different phenotypes of nonproliferative diabetic retinopathy (NPDR) and their progression to clinically significant macular edema (CSME).

Methods. A prospective observational study was designed to follow eyes/patients with diabetes type 2 and NPDR with no prior laser treatment for 2 years or until development of CSME. A total of 410 patients, one eye per patient, fulfilled the inclusion/exclusion criteria and were included in the study. Ophthalmological examinations, including BCVA, fundus photography with Retmarker analysis, and optical coherence tomography (OCT), were performed at baseline, month 6 and month 24, or before laser treatment. Hierarchical cluster analysis was used to identify homogeneous subgroups and clinically significant thresholds of the data collected.

Results. A total of 376 eyes/patients performed the 6-month visit and were considered for cluster analysis. This mathematical method identified three different phenotypes based on statistically significant differences for the microaneurysm (MA) turnover and for the central retinal thickness (RT): phenotype A (low MA turnover and normal RT, 48.1%); phenotype B (low MA turnover and increased central RT, 23.2%); and phenotype C (high MA turnover, 28.7%). From the 348 eyes/patients that reached the study end point or completed the 24-month visit, 26 developed CSME: 3 from phenotype A (1.8%), 7 from phenotype B (8.5%), and 16 from phenotype C (16.2%). Eyes/patients from phenotype C showed a higher risk for CSME development (OR = 3.536; $P < 0.001$).

Conclusions. Hierarchical cluster analysis identifies three different phenotypes of NPDR based on MA turnover and central macular thickness. Eyes/patients from phenotype C show a higher risk for the development of CSME. (ClinicalTrials.gov number, NCT00763802.)

Keywords: cluster analysis, phenotypes, diabetic retinopathy

Diabetic retinopathy (DR) is a common and serious ophthalmic condition. It is the leading cause of blindness among working-age adults in the United States.[1] Vision loss related to eye disease among people with diabetes is an important disability that threatens independence and can lead to reduced quality of life.[2]

Furthermore, a recent study by Narayan et al.[3] demonstrated that diabetes prevalence in the United States is likely to increase dramatically through 2050, given recent increases in the incidence of diagnosed diabetes, decreases in diabetes-related mortality, and expected changes in the age of the population. This perspective is perceived to occur in other regions of the world.[4]

It is well recognized that the duration of diabetes and the level of metabolic control condition the development of the retinopathy, but these risk factors do not explain the great variability that characterizes the evolution and rate of progression of the retinopathy in different diabetic patients. There are many diabetic patients who after many years with diabetes never developed sight-threatening retinal changes, maintaining good visual acuity. However, there are also other patients that even after only a few years of diabetes show a retinopathy that progresses rapidly and may not even respond to available treatments.

In a prospective 3-year follow-up study of 14 patients with type 2 diabetes and mild nonproliferative diabetic retinopathy (NPDR) followed using multimodal macula mapping, we found marked individual variations in the progression of DR and activity of retinal disease.[5] In this study, we were able to identify three major patterns of DR progression. The first one, identified as pattern A, consisted of eyes in which the retinal changes progressed slowly and showed little disease activity over the 3-year period of follow-up. The second, identified as pattern B, or wet form, was characterized by alterations of the blood-retinal barrier and the presence of edema. The third, identified as pattern C, or ischemic form, was characterized by increased retinal vascular remodeling and capillary closure. These different phenotypes were associated with different risks for DR worsening and development of clinically significant macular edema (CSME). Shortcomings of this study were the elaborate imaging methodology used and the small sample size.

In this study, we report the identification of similar phenotypes based on hierarchical cluster analysis in a prospective study of a large cohort of type 2 diabetic patients

with mild NPDR using only noninvasive imaging methodologies that are easily used in routine clinical practice, digital color fundus photography (CFP), and optical coherence tomography (OCT) and their 2-year progression to CSME.

Methods

Patients

The study was a prospective, observational study designed to follow eyes/patients with mild NPDR (20 and 35 of Early Treatment Diabetic Retinopathy Study [ETDRS] classification) for a period of 2 years or until the time of development of CSME needing treatment.

A total of 410 patients were included between September 2007 and December 2009, men and women with diagnosed adult-onset type 2 diabetes, age 40 to 75 years, mild NPDR (20 and 35 of ETDRS classification), best corrected visual acuity (BCVA) as tested in the ETDRS[6] of 80 or higher ETDRS letters score (Snellen equivalent $\geq$20/25) and refraction with a spherical equivalent less than $\pm$5 diopters (D). Exclusion criteria included the presence of cataract or other eye disease that may interfere with fundus examination, glaucoma, other retinal disease, previous intraocular surgery, dilatation of the pupil less than 5 mm and previous laser therapy or intravitreal injections. All patients gave written informed consent. The tenets of the Declaration of Helsinki were followed and approval was obtained from the institutional review board (clinical trial registration number: NCT00763802).

At the baseline visit (V0) patients' body weight, height, blood pressure, and concomitant medication were recorded. A physical examination by a diabetologist was also performed.

One eye per patient was selected by the physician at baseline as the study eye based on the inclusion/exclusion criteria. When both eyes fulfilled the same criteria, one of the eyes was selected by choosing sequentially the right or the left eye.

At the three study visits, V0, V6, and V24 (or pretreatment visit), the study eyes underwent a complete eye examination, which included BCVA, slit-lamp examination, IOP measurements, digital CFP, and OCT.

During the period of the study and outside of the study visits, patients were followed in our institution according to usual clinical practice. Patients diagnosed as having CSME (identified on clinical examination by retinal thickening within 500 μm of the center of the fovea or by the presence of exudates within 500 μm of the center of the fovea, or by adjacent thickening or thickening of at least 1 disc area of any part within 1 disc diameter of the center of the fovea[7]) were referred to the principal investigator of the study (JC-V) for a full visit before treatment. Laser photocoagulation treatment for CSME was the first choice treatment at the time when the study was performed.

Laboratory analyses were performed at baseline (V0) and at the 6-month (V6) and at the 24-month (V24) visits or at the pretreatment visit. Laboratory analyses included creatinine, glucose and HbA_{1C} concentration, red blood cell count, white blood cell count, platelet amount, hemoglobin concentration, and packed cell volume. Metabolic control was also assessed by measuring in the plasma concentrations of lipid fractionation identifying total cholesterol, high-density lipoprotein (HDL), low-density lipoprotein (LDL), and triglycerides.

Baseline characteristics are presented in Table 1.

Table 1. Baseline Characteristics for the Patients Included in the Study ($n = 410$)

	Patients Included in the Study, $n = 410$
Males/Females, frequency (%)	259 (63.2)/151 (36.8)
Taking insulin, yes/no, frequency (%)	117 (28.5)/293 (71.5)
Age, y	62.0 (55.0–67.0)
Duration of diabetes, y	10.0 (6.0–14.0)
Creatinine, mg/dL	0.89 (0.78–1.01)
HbA_{1C}, %	7.7 (6.9–8.9)
Cholesterol, mg/dL	194 (168–222)
HDL, mg/dL	49 (42–58)
LDL, mg/dL	125 (105–148)
Glucose, mg/dL	165 (119–226)
Triglycerides, mg/dL	145 (104–214)
Systolic blood pressure, mm Hg	151 (136–164)
Diastolic blood pressure, mm Hg	76 (69–82)
BCVA, letters	85 (83–89)
No. of MAs	2 (1–5)
Central subfield retinal thickness, central 1000 μm, μm	215.5 (198.0–233.0)

Values are median and IQR, or frequency and percentage.

Color Fundus Photography

CFP was performed according to the ETDRS protocol. The seven-fields photographs were obtained at 30° using a Zeiss FF450 camera (Carl Zeiss Meditec, Dublin, CA) for DR classification according to ETDRS grading.

The field-2 images were subjected to automated microaneurysm (MA) analyses using the RetmarkerDR (Critical Health SA, Coimbra, Portugal). This automated computer-aided diagnostic system consists of software earmarking MA and vascular lesions in the macula; it includes a coregistration algorithm that allows comparison within the same retinal location between different visits for the same eye.[8,9] The algorithm detects the presence of MA and red dotlike lesions (i.e., small lesions that appeared as a round or ovoid red spot of 20–200 μm in diameter with regular borders and located within the superior and inferior arcades).

The RetmarkerDR computes for each eye/patient the number of MAs in each visit, the number of MAs that appear and/or disappear from one visit to the other, allowing calculation of the number of MAs appearing and/or disappearing per time interval (i.e., the MA formation rate and the MA disappearance rate, respectively). The MA turnover is computed as the sum of the MA formation and disappearance rates.

In a previous work from our group,[10,11] a good intergrader agreement was found for the total number of MAs earmarked and the MA turnover for three independent human graders. The RetmarkerDR shows a similar intergrader agreement for the total number of MAs and the MA turnover while showing no intragrader variability as opposed to human graders being, therefore, a reliable tool for MA assessment.[12]

Optical Coherence Tomography

OCT was performed using the Stratus-OCT (Carl Zeiss Meditec).

The *Fast Macular* acquisition protocol, acquiring six radial scans 30° apart, 6 mm long, was used to assess the central retinal thickness (RT).

Due to the strong correlation found between the central point RT and the central subfield RT ($r = 0.948$; $P < 0.001$), and due to the higher variability found in central point RT measurements,[13] only the central subfield RT was considered in this study.

Data Analysis

Patients are usually characterized by estimated values of the parameters under analysis (e.g., mean or median values). To analyze the homogeneity of the distribution of the data, dispersion measures of the parameters considered can be used (e.g., coefficient of variation when using the mean or coefficient of dispersion when using the median). The higher the measures of dispersion, the more heterogeneity the group of patients analyzed has.

Cluster analysis is a mathematical method that, based on the data dispersion observed in a group of patients, identifies more homogeneous subgroups (i.e., smaller groups of patients with the lowest dispersion). Cluster analyses are therefore unsupervised segmentation techniques that build models of the observed data in order to identify and create homogeneous groups.[14] These techniques group data that share some similarity measure or feature,[15] being hierarchical or nonhierarchical (i.e., when the number of underlying clusters is unknown or known a priori). In this work, the hierarchical method was used to identify the number of homogeneous groups (clusters) underlying the data set.

The Ward's method was used for hierarchical clustering. This method creates clusters by agglomeration (i.e., starting by considering initially the existence of as many clusters as patients and keeping agglomerating clusters until it achieves a single one enclosing all of the patients). Ward's method promotes the minimization of the within-cluster dispersion being therefore one of the methods more frequently used in clinical sciences.[16–18] Along the agglomerative process, the dissimilarity measure between the grouped clusters is computed. The analysis of this dissimilarity measure along the agglomeration process allows the number of homogeneous clusters in the data set to be identified. Moreover, to determine the best number of clusters, the Calinsky-Harabasz pseudo-F statistic was also computed.[19]

To identify phenotypes of mild NPDR using noninvasive procedures, a hierarchical Ward's cluster analysis was performed using MA parameters (number of MA at baseline and MA turnover from baseline to month 6) and central subfield RT parameters (central subfield RT at baseline and changes from baseline to month 6). Since the range of values for the different parameters had one order of magnitude, a data normalization was performed before clustering. In this way, the normalization was achieved through a *Z*-distribution, thus having a zero mean and unitary standard deviation (*Z*-score values).

The identified clusters (i.e., phenotypes) were thereafter fully characterized, based on the original parameters and on the remaining parameters: age, diabetes duration, creatinine, HbA_{1C}, blood pressure, cholesterol, HDL, LDL, glucose, and triglyceride levels. Statistically significant differences between phenotypes were tested using the Kruskall-Wallis test. The risk for CSME development (odds ratio [OR]) was computed and compared between the identified phenotypes of mild NPDR.

Once the phenotypes were identified (based on the cluster analysis), a decision and classification tree was used to establish rules for phenotype classification. This method allows for the establishment of rules based on cut-off values.

Statistical analyses were performed using the STATA software version 12.1 (StataCorp LP, College Station, TX), and *P* values less than or equal to 0.05 were considered as statistically significant results.

To identify threshold values for the phenotypes, a decision and classification tree was performed using the parameters considered in the cluster analysis. The CART algorithm with a 10-fold cross-validation was used (SPSS version 13.0; IBM SPSS, Inc., Chicago, IL).

Results

From the 410 eyes/patients included in the study, 376 completed the first 6 months of follow-up (2 patients died between the baseline and the 6-month visit, 25 withdrew from the study, and 7 were lost to follow-up). Only 348 eyes/patients reached either the study end point, CSME needing treatment (26 eyes/patients), or performed the last study visit (24-month visit) without developing CSME (322). There were a total of 62 dropouts from the study (9 patients died, 44 withdrew from the study, and 9 were lost to follow-up) (Fig. 1). Of the 348 eyes/patients that completed the study 15 eyes (4.3%) progressed to more advanced ETDRS levels: 14 progressed to moderate NPDR (11 with level 43A and 3 with level 43B), and 1 progressed to moderate proliferative DR (level 65B). No statistically significant differences were found between the 348 eyes/patients that reached the study end point or that performed the last study visit and the 62 eyes/patients that dropped out, except for the cholesterol, the LDL levels, and the BCVA (Table 2).

For the cluster analysis, based on the MA and RT parameters, the 376 eyes/patients that performed the 6-month visit were considered.

Furthermore, to assess increased retinal thickness an age-matched healthy population was used. The normal mean and SD for the central subfield RT were 201.1 ± 18.9 μm. No statistically significant differences were found between sexes (the mean central subfield RT for males was 201.8 ± 15.4 μm and for females 201.4 ± 21.8 μm; $P > 0.05$).

Phenotypes of Mild NPDR

The hierarchical Ward's clustering method identified the existence of three clusters, corresponding to the higher Calinsky-Harabasz pseudo-*F* statistics (Fig. 2) (for the three clusters solution the Calinsky-Harabasz pseudo-*F* statistics was 91.9, whereas for the four clusters solution the Calinsky-Harabasz pseudo-*F* statistics was 69.7). The first cluster/phenotype was composed of 181 eyes/patients (48.1%), the second cluster/phenotype was composed of 87 eyes/patients (23.2%), and the third cluster/phenotype was composed of 108 eyes/patients (28.7%).

The three phenotypes result from the statistically significant differences for the MA and the RT parameters ($P < 0.001$, Table 3). Statistically significant differences between phenotypes were also found for sex ($P = 0.028$), age ($P < 0.001$), HbA_{1C} ($P = 0.050$) and LDL levels ($P = 0.049$), and for the BCVA ($P = 0.001$) (Table 3).

Phenotype B is characterized by a higher central subfield RT ($P < 0.001$). This phenotype shows a lower BCVA ($P < 0.027$, corresponding only to one ETDRS letter difference) and is composed mainly of males ($P = 0.015$ when compared with phenotype A) and older subjects ($P < 0.011$). Phenotype C is characterized by higher MA parameters, number, and turnover ($P < 0.001$). This phenotype also showed higher HbA_{1C} values ($P = 0.043$ when compared with phenotype A) and lower LDL values ($P < 0.038$).

Representative cases for the three phenotypes are shown in Figure 3.

Phenotypes of Mild NPDR and Risk for CSME

From the 348 eyes/patients that reached the study end point or that completed the 24-month visit, 26 developed CSME needing laser photocoagulation, 3 (1.8%) from phenotype A, 7 (8.5%) from phenotype B, and 16 (16.2%) from phenotype C (Fig. 4).

CSME eye/patient characteristics are shown in Table 4. Statistically significant differences between eyes/patients that did not develop CSME and eyes/patients that developed CSME

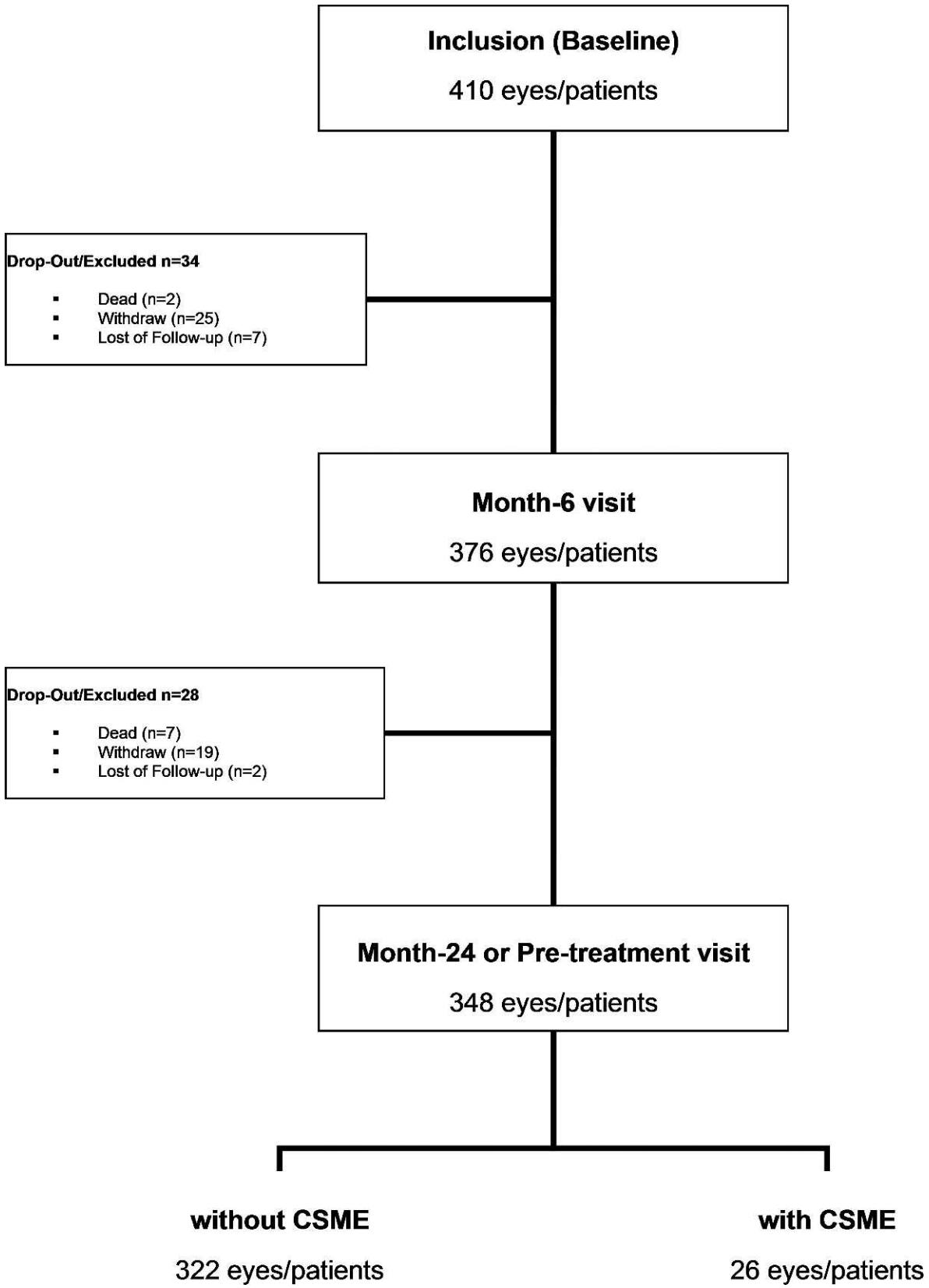

FIGURE 1. Composition of the patients included in the study over the study period: CONSORT flowchart.

Investigative Ophthalmology & Visual Science

Table 2. Baseline Characteristics of the Eyes/Patients That Reached the Study End Point or That Performed the Last Study Visit

	Drop–Out Patients, $n = 62$	Patients Included in the Analysis, $n = 348$	P
Males/females	41 (65.1)/22 (34.9)	219 (62.9)/129 (37.1)	NS
Age, y	63.5 (58.0–69.0)	62.0 (55.0–67.0)	NS
Duration of diabetes, y	10.0 (5.0–14.0)	10.0 (6.0–14.0)	NS
Patients taking insulin	14 (22.6)	103 (29.6)	NS
Creatinine, mg/dL	0.89 (0.79–1.02)	0.89 (0.78–1.01)	NS
HbA_{1C}, %	7.9 (6.5–9.0)	7.7 (6.9–8.9)	NS
Cholesterol, mg/dL	208.5(173.0–228.0)	193.0 (167.0–219.0)	0.016
HDL, mg/dL	51.5 (43.0–59.0)	49.0 (42.0–57.0)	NS
LDL, mg/dL	132.0 (108.0–156.0)	124.0 (105.0–146.0)	0.010
Glucose, mg/dL	168.5 (113.0–230.0)	163.0 (119.0–226.0)	NS
Triglycerides, mg/dL	132.0 (104.0–192.0)	147.0 (104.0–220.0)	NS
Systolic blood pressure, mm Hg	152.0 (135.0–170.0)	151.0 (137.0–164.0)	NS
Diastolic blood pressure, mm Hg	75.0 (72.0–82.0)	76.0 (69.0–82.5)	NS
BCVA, letters	84 (80–88)	85 (84–89)	0.010
No. of MAs	2 (1–6)	2 (1–5)	NS
Central subfield RT, central 1000 μm, μm	211 (192–229)	216 (199–233)	NS

Values are median and IQR, or frequency and percentage; P value for statistically significant differences between eyes/patients.
NS, not significant, $P > 0.05$.

were found only for the MA parameters ($P \leq 0.002$) and for the RT parameters ($P \leq 0.035$).

Eyes/patients from phenotypes C and B showed a higher risk for CSME than eyes/patients from phenotype A. For phenotype C, the OR is 3.536, 95% confidence interval (CI) 1.917–6.524 ($P < 0.001$); and for phenotype B the OR is 2.802, 95% CI 1.445–5.434 ($P = 0.002$). Phenotype C shows also a higher risk for CSME when compared with phenotype B (the OR is 1.994, 95% CI 1.144–3.477; $P = 0.015$).

Threshold Values for Phenotypes

Based on the three phenotypes, threshold values were identified using a decision and classification tree (Fig. 5): 73.5% of the eyes/patients in phenotype A (133 of the 181 eyes/patients) were characterized by an MA turnover less than 6 and a central RT less than 217 μm; 98.8% of the eyes/patients in phenotype B (86 of the 87 eyes/patients) were characterized by an MA turnover less than 6 and a central RT greater than or equal to 217 μm; 97.2% of the eyes/patients in phenotype C (105 of the 108 eyes/patients) were characterized by an MA turnover greater than or equal to 6.

The resulting classification tree presents a risk estimate of 12.5%, classifying correctly 88.6% of the eyes/patients in one of the three phenotypes.

Considering these thresholds, and based on the clinically meaningful parameters, that is, MA turnover and presence of edema (i.e., central RT increase over the normal reference

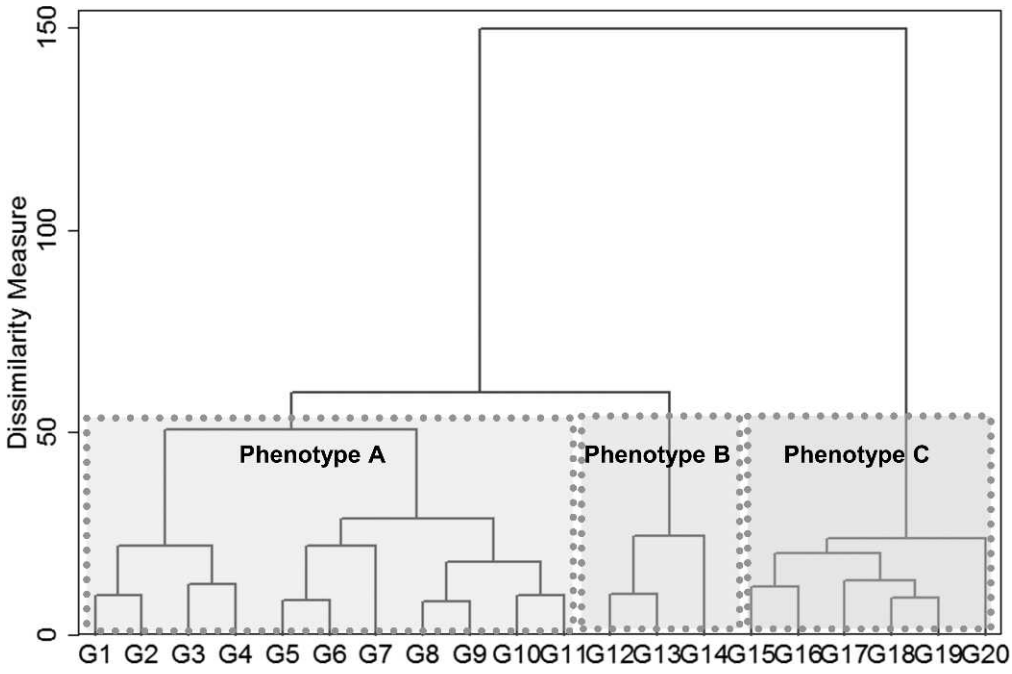

Figure 2. Dendrogram for the Ward's clustering method showing the dissimilarity measure that is computed in each iteration of the hierarchical agglomerative process (the clustering starts with 376 clusters, i.e., as many groups as eyes/patients, and ended with one single cluster). To simplify the graphical representation, the dissimilarity measures are shown from the 20 clusters solution (G1 to G20).

Table 3. Characteristics of Each Phenotype ($n = 376$)

	Phenotype A $n = 181$	Phenotype B $n = 87$	Phenotype C $n = 108$	*P*
Males/females, frequency (%)	101 (55.8)/80 (44.2)	62 (71.3)/25 (28.7)	72 (66.7)/36 (33.3)	**0.028**
Taking insulin, yes/no, frequency (%)	50 (27.6)/131 (72.4)	30 (34.5)/57 (65.5)	31 (28.7)/77 (71.3)	0.502
Age, y	62 (54–68)	64 (59–70)	59 (53–65)	**<0.001**
Duration of diabetes, y	10 (6–13)	10 (6–15)	10 (6–14)	0.645
Creatinine, mg/dL	0.89 (0.78–1.01)	0.90 (0.80–1.03)	0.87 (0.76–1.01)	0.279
HbA_{1C}, %	7.7 (6.7–8.8)	7.6 (6.9–9.0)	7.9 (7.0–9.1)	**0.050**
Cholesterol, mg/dL	196 (169–218)	200 (177–222)	182 (161–215)	0.058
HDL, mg/dL	49 (42–57)	50 (41–58)	48 (42–56)	0.909
LDL, mg/dL	127 (107–148)	128 (110–149)	116 (101–136)	**0.049**
Glucose, mg/dL	165 (118–226)	166 (110–219)	162 (127–226)	0.742
Triglycerides, mg/dL	157 (109–236)	145 (106–208)	138 (99–189)	0.088
Systolic blood pressure, mm Hg	153 (136–166)	149 (141–165)	148 (134–159)	0.159
Diastolic blood pressure, mm Hg	75 (68–82)	75 (70–82)	76 (69–83)	0.783
BCVA, letters	85 (83–89)	84 (82–88)	87 (84–89)	**0.001**
No. of MAs	3 (1–4)	1 (1–2)	9 (6–12)	**<0.001**
MA turnover, no. per 6 mo	3 (1–5)	1 (0–2)	9 (7–14)	**<0.001**
Central subfield RT, central 1000 μm, μm	204 (192–212)	234 (227–245)	218 (198–235)	**<0.001**
Central subfield RT at month 6, central 1000 μm, μm	204 (190–219)	235 (222–247)	216 (202–231)	**<0.001**

Values are median and IQR, or frequency and percentage; *P* values for the three phenotypes (bold indicates values that are statistically significant).

value, 201.1 ± 18.9 μm), the following rules can be used to classify eyes/patients into one of the three phenotypes of NPDR progression:

- Phenotype A: MA turnover < 6 and normal RT values (central subfield RT < 220 μm, i.e., normal mean + 1 SD).
- Phenotype B: MA turnover < 6 and increased RT values (central subfield RT ≥ 220 μm).
- Phenotype C: MA turnover ≥ 6.

From the 133 eyes/patients with an MA turnover less than 6 and a central RT less than 220 μm, 1 eye/patient developed CSME (0.7%); from the 94 eyes/patients with an MA turnover less than 6 and a central RT greater than or equal to 220 μm, 8 eyes/patients developed CSME (8.5%); and from the 121 eyes/patients with an MA turnover greater than or equal to 6, 17 eyes/patients developed CSME (14.5%).

Using these rules to estimate the risk for CSME development, phenotype B shows a sensitivity and a specificity of 88.9% and 60.5%, respectively (when compared to phenotype A), and phenotype C shows a sensitivity and a specificity of 94.4% and 55.9%, respectively (when compared to phenotype A).

Phenotype A shows a negative predictive value for developing CSME of 99.2%.

Discussion

The aim of this study was to identify patterns of progression and retinal disease activity in patients with diabetes type 2 and NPDR with noninvasive procedures used in routine clinical practice.

This study shows that using the mathematical method of hierarchical cluster analysis and only noninvasive procedures (CFP and OCT), three different phenotypes of NPDR can be identified, which show different risks of progression to CSME.

These three phenotypes are in agreement with the number of patterns of DR progression proposed previously by Lobo et al.[5] in a different and smaller sample. In this original study, three phenotypes of progression of mild NPDR were characterized: phenotype A as slow progression, phenotype B as "leaky," and phenotype C as ischemic. Similar categorization was found in this study as a result of hierarchical cluster analysis, phenotype B with predominance of edema, and phenotype C with predominance of MA turnover (i.e., with increased rates of MA formation and disappearance).

The main initial alterations occurring in the early stages of NPDR are MA formation and disappearance, capillary closure, and alteration of the blood-retinal barrier with associated retinal edema.[20] Digital CFP and OCT alone, both noninvasive procedures, appear to be adequate to document these initial alterations. MA and small hemorrhages can be detected by CFP, and their turnover (i.e., disease activity) can be quantified using a novel software for automatic analysis of the fundus images, the RetmarkerDR. MA turnover is a composite of MA formation rate, that is, the number of new MA per time interval and MA disappearance rate (i.e., number of disappearing MA per time interval). Both parameters represent microvascular disease activity and more specifically, the MA disappearance rate is considered a sign of capillary closure.

On the other hand, increased retinal thickness quantified by OCT identifies the presence of edema, which is a direct result of the alteration of the blood-retinal barrier. Fluorescein angiography was not used because the aim of the study was to identify patterns of progression using noninvasive procedures that can be easily repeated in clinical practice.

It was striking to find that 348 eyes/patients with similar levels of ETDRS classification (20–35) showed such a large interquartile range (IQR) both in MA turnover and retinal thickness values, demonstrating the wide range of values for each of these alterations. Hierarchical cluster analysis showed that these initial changes occur in different levels of intensity in different groups of patients and that different groups of patients can be characterized by levels of intensity of these retinal changes.

Our findings show that increased activity of microvascular disease in the macular region (field 2), well demonstrated by increased rates of MA turnover that characterize phenotype C, is associated with higher risk for development of CSME in the relatively short period of 2 years. This phenotype represents approximately 30% of the patients.

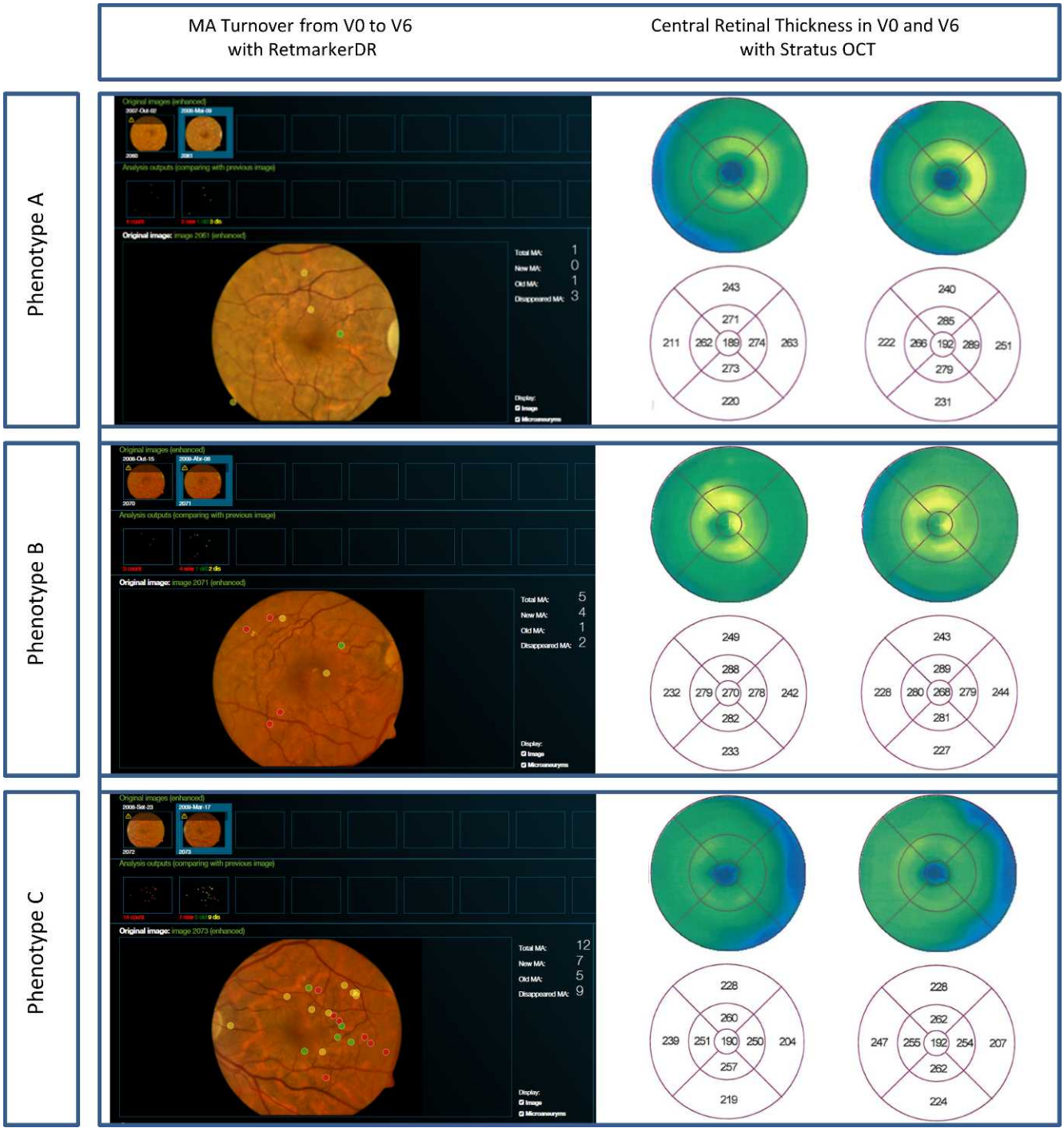

Figure 3. Representative cases for the three phenotypes of DR progression (*right side*: color fundus image in V6 with the MA earmarked using the software RetmarkerDR: *red dots* are new MA, *yellow dots* are MA that disappeared from V0 to V6, and *green dots* are MA that were present in both visits; *left side*: central macular thickness maps obtained with the Stratus OCT in V0, *left*, and in V6, *right*). Phenotype A images are from case 007 (OD), the MA Turnover (number of MA appearing plus number of MA disappearing) was 3 MA in 6 months and the central retinal thicknesses in V0 and V6 were 180 μm and 192 μm, respectively. This patient had a BCVA of 84 letters at baseline. Phenotype B images are from case 104 (OD), the MA Turnover was 6 MA in 6 months and the central retinal thicknesses in V0 and V6 were 270 μm and 268 μm, respectively. This patient had a BCVA of 82 letters at baseline. This patient developed CSME 6 months after V6. Phenotype C images are from case 210 (OS), the MA Turnover was 16 MA in 6 months and the central retinal thicknesses in V0 and V6 were 190 μm and 192 μm, respectively. This patient had a BCVA of 84 letters at baseline. This patient developed CSME in the last study visit.

Of relevance is also the finding that on the other hand, phenotype A, which is characterized by low MA turnover and also no signs of retinal edema (representing approximately 50% of the patients), has the lowest risk for development of CSME, predictive negative value of 99.2%. This observation has clear implications for management of DR. Furthermore, this observation indicates that a large proportion of the eyes with mild NPDR will progress very slowly, suggesting that these

Investigative Ophthalmology & Visual Science

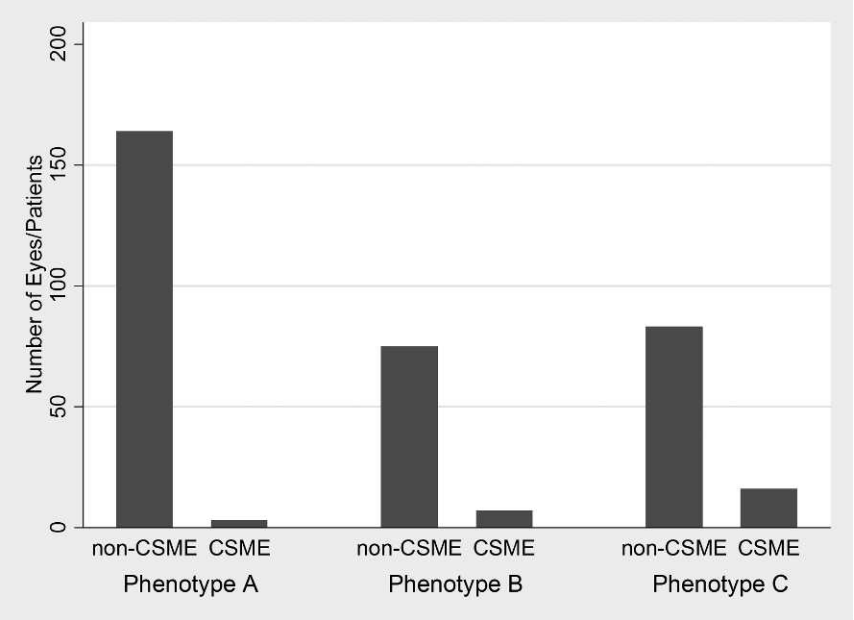

FIGURE 4. Phenotypes distribution by non-CSME and CSME eyes (number of eyes/patients for each phenotype that completed the 24-month visit without developing CSME – non-CSME, and number of eyes/patients for each phenotype that developed CSME needing treatment – CSME).

eyes should not be included in clinical trials because of their slow rates of progression. New OCT methodologies, such as swept-source OCT or even Doppler OCT, have the potential to achieve finer characterization of the different DR phenotypes.

Various systemic risk factors have been proposed to influence progression of DR. Our study shows that progression to CSME from the initial stages of the retinopathy is apparently mainly correlated with HbA_{1C} (i.e., glycemic metabolic control). Blood pressure measurements did not show any correlation with the risk for development of CSME, and from the creatinine and blood lipids levels analyzed, only LDL showed a correlation: lower LDL values are present in phenotype C. It appears that these risk factors may play a role only in more advanced stages of the disease when vision-threatening complications, such as CSME and proliferative retinopathy, are present.

It is of note that phenotype C was identified in a younger population. Because the duration of diabetes was similar in the three phenotypes suggests that eyes/patients with earlier onset of their diabetes have increased activity of their microvascular disease, which characterizes phenotype C.

The identification of different retinopathy phenotypes characterized by different dominant retinal alterations and different rates of progression to CSME opens new perspectives for personalized management of DR. If the patients with the greatest risk of progression and with the greatest potential to benefit from treatment can be identified, fewer patients will need to be followed closely to prevent one case of blindness.

TABLE 4. Characteristics of the Eyes/Patients That Did Not Develop CSME ($n = 322$) and That Developed CSME ($n = 26$)

	Eyes/Patients That Did Not Develop CSME, $n = 322$	Eyes/Patients That Developed CSME, $n = 26$	P
Males/females, frequency (%)	204 (63.3)/118 (36.7)	15 (57.7)/11 (42.3)	0.565
Taking insulin, yes/no, frequency (%)	94 (29.2)/228 (70.8)	9 (34.6)/17 (65.4)	0.560
Age, y	62 (55–67)	63 (54–70)	0.341
Duration of diabetes, y	10 (6–14)	11 (7–15)	0.281
Creatinine, mg/dL	0.88 (0.78–1.01)	0.89 (0.78–1.00)	0.987
HbA_{1C}, %	7.6 (6.9–8.8)	8.1 (7.3–10.0)	0.071
Cholesterol, mg/dL	193 (167–218)	197 (164–228)	0.850
HDL, mg/dL	49 (42–57)	48 (44–55)	0.809
LDL, mg/dL	124 (104–146)	121 (105–150)	0.743
Glucose, mg/dL	162 (119–225)	171 (128–239)	0.551
Triglycerides, mg/dL	147 (104–220)	142 (112–199)	0.671
Systolic blood pressure, mm Hg	151 (137–164)	147 (135–168)	0.963
Diastolic blood pressure, mm Hg	76 (69–82)	71 (65–84)	0.399
BCVA, letters	85 (84–89)	85 (84–89)	0.454
No. of MAs	3 (1–6)	8 (3–12)	**0.002**
MA turnover, no. per 6 mo	4 (1–7)	9 (3–16)	**<0.001**
Central subfield RT, central 1000 μm, μm	214 (198–233)	227 (208–239)	**0.035**
Central subfield RT at month 6, central 1000 μm, μm	214 (199–231)	226 (212–260)	**0.005**

Values are median and IQR, or frequency and percentage; P values for non-CSME versus CSME eyes/patients (bold indicates values that are statistically significant).

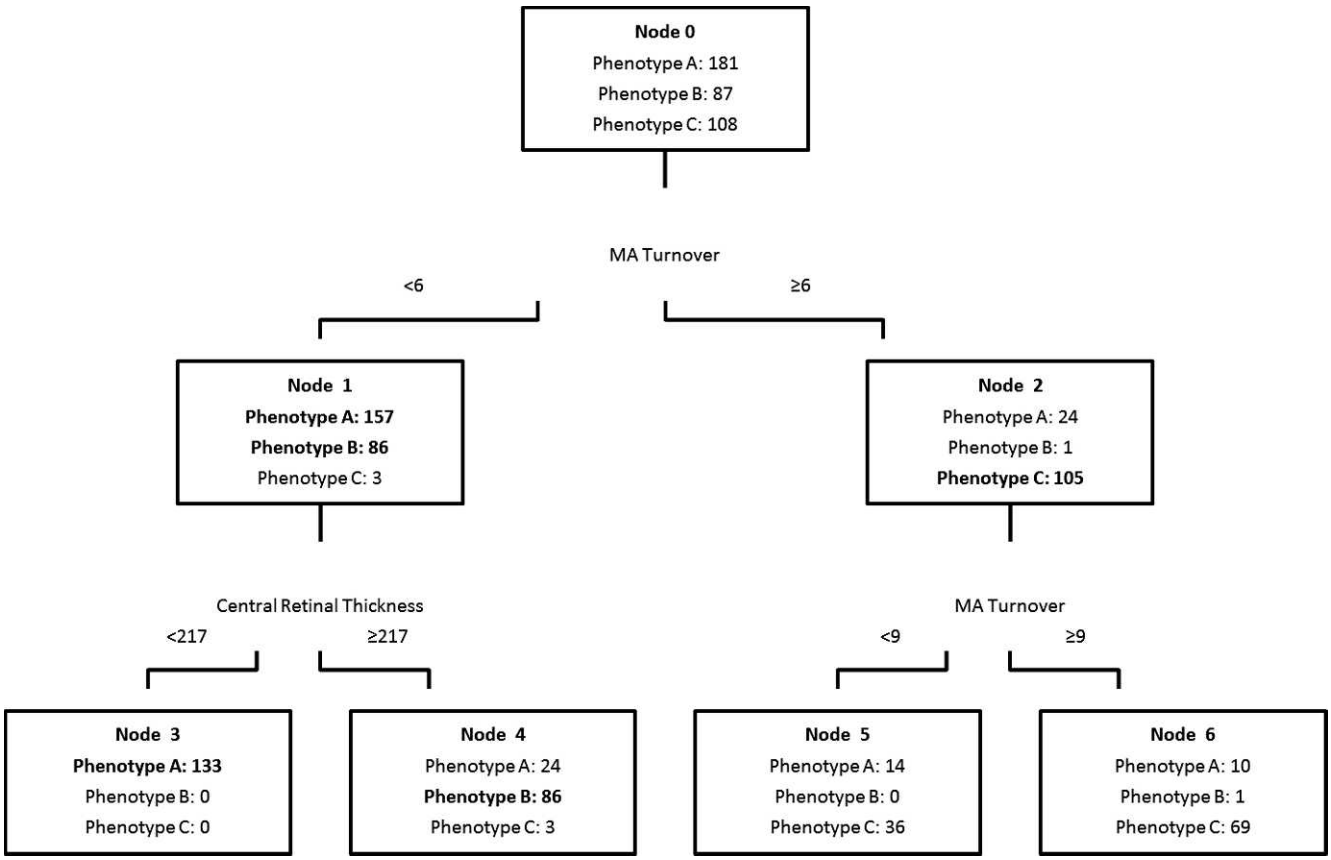

FIGURE 5. Decision and classification tree for the characterization of the three phenotypes. Nodes showing the higher number of eyes/patients from one single phenotype were used for phenotype characterization (for phenotype A characterization node 3 was considered; for phenotype B characterization node 4 was considered; and for phenotype C characterization node 2 was considered).

This is of extreme importance at a time in which scarce resources must be focused and concentrated on the individual cases that need close follow-up and timely treatment.

Limitations of this study are the relatively short duration of the follow-up period, only 2 years, the relatively short number of visits, and the option for noninvasive procedures.

In summary, eyes in the initial stages of DR show three different phenotypes that can be identified by noninvasive procedures and that have different risks for short-term development of CSME.

Acknowledgments

Supported by Fundação para a Ciência e a Tecnologia, Portugal, under the research project PTDC/SAU-OSM/72635/2006 (trial registry NCT00763802, ClinicalTrials.gov).

Disclosure: **S. Nunes**, None; **L. Ribeiro**, None; **C. Lobo**, None; **J. Cunha-Vaz**, None.

References

1. Fong DS, Aiello L, Gardner TW, et al. Retinopathy in diabetes. *Diabetes Care*. 2004;27:S84–S87.
2. Sinclair AJ, Bayer AJ, Girling AJ, Woodhouse KW. Older adults, diabetes mellitus and visual acuity: a community-based case-control study. *Age Ageing*. 2000;29:335–339.
3. Narayan KM, Boyle JP, Geiss LS, Saaddine JB, Thompson TJ. Impact of recent increase in incidence on future diabetes burden: U.S., 2005–2050. *Diabetes Care*. 2006;29:2114–2116.
4. Prokofyeva E, Zrenner E. Epidemiology of major eye diseases leading to blindness in Europe: a literature review. *Ophthalmic Res*. 2012;47:171–188.
5. Lobo CL, Bernardes RC, Figueira JP, Faria de Abreu JR, Cunha-Vaz JG. Three-year follow-up of blood retinal barrier and retinal thickness alterations in patients with type 2 diabetes mellitus and mild nonproliferative retinopathy. *Arch Ophthalmol*. 2004;122:211–217.
6. Plainis S, Tzatzala P, Orphanos Y, Tsilimbaris M. A modified ETDRS visual acuity chart for European-wide use. *Optom Vis Sci*. 2007;84:647–653.
7. Early Treatment Diabetic Retinopathy Study Research Group. Photocoagulation for diabetic macular edema. Early Treatment Diabetic Retinopathy Study report number 1. *Arch Ophthalmol*. 1985;103:1796–1806.
8. Bernardes R, Baptista P, Cunha-Vaz J, Dias J. Multimodal functional and morphological nonrigid image registration. In: *International Conference on Image Processing*. Genoa, Italy: ICIP 2005;1:1133–1136.
9. Ferreira J, Bernardes R, Baptista P, Dias J, Cunha-Vaz J. Earmarking retinal changes in a sequence of digital color fundus photographs. In: *The 3rd European Medical and Biological Engineering Conference*. Prague, Czech Republic: IFMBE 2005;11:1924-1–1924-6.
10. Nunes S, Pires I, Rosa A, Duarte L, Bernardes R, Cunha-Vaz J. Microaneurysm turnover is a biomarker for diabetic retinopathy progression to clinically significant macular edema: findings for type 2 diabetics with nonproliferative retinopathy. *Ophthalmologica*. 2009;223:292–297.

11. Bernardes R, Nunes S, Pereira I, et al. Computer-assisted microaneurysm turnover in the early stages of diabetic retinopathy. *Ophthalmologica*. 2009;223:284–291.
12. Ribeiro L, Nunes S, Cunha-Vaz J. Microaneurysm turnover at the macula predicts risk of development of clinically significant macular edema in persons with mild nonproliferative diabetic retinopathy. *Diabetes Care*. 2013;36:1254–1259.
13. Grover S, Murthy R, Brar V, Chalam K. Comparison of retinal thickness in normal eyes using stratus and spectralis optical coherence tomography. *Invest Ophthalmol Vis Sci*. 2010;51:2644–2647.
14. Everitt B. Commentary: classification and cluster analysis. *BMJ*. 1995;311:535–536.
15. Kaufman L, Rouseeuw P. *Finding Groups in Data: An Introduction to Cluster Analysis*. New York: John Wiley & Sons, Inc.; 1990.
16. Mathers W, Dongseok C. Cluster analysis of patients with ocular surface disease, blepharitis, and dry eye. *Arch Ophthalmol*. 2004;122:17000–17004.
17. Rosenberg D, Handler A, Furner S. A new method for classifying patterns of prenatal care utilization using cluster analysis. *Maternal Child Health J*. 2004;8:19–30.
18. Baek S, Sung KR, Sun JH, et al. A hierarchical cluster analysis of primary angle closure classification using anterior segment optical coherence tomography parameters. *Invest Ophthalmol Vis Sci*. 2013;54:848–853.
19. Milligan W, Cooper M. An examination of procedures for determining the number of clusters in a dataset. *Psychometrika*. 1985;50:159–179.
20. Cunha-Vaz J, Bernardes R. Nonproliferative retinopathy in diabetes type 2. Initial stages and characterization of phenotypes. *Prog Retin Eye Res*. 2005;24:355–377.

Investigative Ophthalmology & Visual Science